Available online at www.sciencedirect.com
SCIENCE DIRECT®
Engineering Applications of Artificial Intelligence 18 (2005) 317–334
Engineering Applications of
ARTIFICIAL
INTELLIGENCE
www.elsevier.com/locate/engappai

Stable auto-tuning of hybrid adaptive fuzzy/neural controllers for nonlinear systems

Hazem N. Nounou[a,*], Kevin M. Passino[b]

[a]Department of Electrical Engineering, United Arab Emirates University, P.O. Box 17555, Al-Ain, UAE
[b]Department of Electrical Engineering, The Ohio State University, 2015 Neil Avenue, Columbus, OH 43210-1272, USA

Received 22 January 2004; received in revised form 12 September 2004; accepted 13 September 2004
Available online 11 November 2004

Abstract

In direct adaptive control, the adaptation mechanism attempts to adjust a parameterized nonlinear controller to approximate an ideal controller. In the indirect case, however, we approximate parts of the plant dynamics that are used by a feedback controller to cancel the system nonlinearities. In both cases, "approximators" such as linear mappings, polynomials, fuzzy systems, or neural networks can be used as either the parameterized nonlinear controller or identifier model. In this paper, we present an algorithm to tune the adaptation gain for a gradient-based hybrid update law used for a class of nonlinear continuous-time systems in both direct and indirect cases. In our proposed algorithm, the adaptation gain is obtained by minimizing the instantaneous control energy. Finally, we will demonstrate the performance of the algorithm via a wing rock regulation example.

Keywords: Adaptive control; Adaptation gain; Fuzzy/neural control

1. Introduction

In adaptive control, the adaptive law is usually used to approximate either the parameters of the ideal controller as in the direct case, or the parameters of the plant dynamics as in the indirect case. Some research has been done in this field for both discrete (Chen and Khalil, 1995) and continuous-time systems (Ioannou and Sun, 1996; Spooner and Passino, 1996). In Chen and Khalil (1995), the authors presented an indirect adaptive control law for a class of feedback linearizable discrete-time nonlinear systems, and provided global results with respect to the state, but local with respect to the parameters. Using the class of systems considered in Chen and Khalil (1995), algorithms to auto-tune the adaptation gain and direction of descent for both direct and indirect adaptive controllers have been presented in Nounou and Passino (2004). In Spooner and Passino (1996), the authors presented both indirect and direct adaptive control algorithms using linearly parameterized approximators to control SISO systems with guaranteed convergence of the tracking error to zero. For this class of systems, an algorithm to auto-tune the direction of the search vector for direct adaptive control systems has been presented in Nounou (2003). Here, this work is extended to auto-tune the adaptation gain for both direct and indirect adaptive control systems. In all of the above cases, the auto-tuning algorithms are based on minimizing the instantaneous control energy which is of great interest in many applications. The paper is organized as follows. In Section 2, direct and indirect adaptive control algorithms are discussed along with a description of the plant considered for control. In Section 3, the hybrid adaptive law used for parameter adaptation and its stability results are discussed. Then, in Section 4, an algorithm to auto-tune the adaptation gain for both direct and indirect adaptive control is presented. Stability results for the auto-tuning algorithm

*Corresponding author. Tel.: +971 37051761; fax: +971 37623156.
E-mail addresses: hnounou@uaeu.ac.ae (H.N. Nounou), passino@ee.eng.ohio-state.edu (K.M. Passino).

0952-1976/$ - see front matter © 2004 Elsevier Ltd. All rights reserved.
doi:10.1016/j.engappai.2004.09.005

are also discussed. In Section 5, an aircraft wing rock simulation is used to illustrate the algorithm. Finally, Section 6 outlines some concluding remarks.

2. Direct and indirect adaptive control

In this section, we start by describing the system we consider for control, along with its assumptions. Then, both direct and indirect adaptive control schemes are briefly discussed, and the error equation is derived for both cases.

2.1. Plant description

Here, we will consider the single-input single-output continuous-time system described by

$$\dot{X} = f(X) + g(X)u_p,$$
$$y_p = h(X), \tag{2.1}$$

where $X \in \Re^n$ is the state vector, $u_p \in \Re$ is the input, $y_p \in \Re$ is the output of the plant and functions $f(X), g(X) \in \Re^n$, and $h(X) \in \Re$ are smooth. If the system has "strong relative degree" r, then it can be shown (as in Spooner and Passino (1996)) that

$$\dot{\xi}_1 = \xi_2 = L_f h(X),$$

$$\vdots$$

$$\dot{\xi}_{r-1} = \xi_r = L_f^{r-1} h(X),$$

$$\dot{\xi}_r = L_f^r h(X) + L_g L_f^{r-1} h(X) u_p \tag{2.2}$$

with $\xi_1 = y_p$, which may be rewritten as

$$y_p^{(r)} = (\alpha_k(t) + \alpha(X)) + (\beta_k(t) + \beta(X))u_p, \tag{2.3}$$

where $L_g^r h(X)$ is the rth Lie derivative of $h(X)$ with respect to g ($L_g h(X) = (\partial h/\partial X)g(X)$, and e.g. $L_g^2 h(X) = L_g(L_g h(X))$), and it is assumed that for some $\beta_0 > 0$, we have $|\beta_k(t) + \beta(X)| \geqslant \beta_0$ so that it is bounded away from zero (for convenience we assume that $\beta_k(t) + \beta(X) > 0$, however, the following analysis may easily be modified for systems which are defined with $\beta_k(t) + \beta(X) < 0$). We will assume that $\alpha_k(t)$ and $\beta_k(t)$ are known components of the dynamics of the plant (that may depend on the state) or known exogenous time dependent signals and that $\alpha(X)$ and $\beta(X)$ represent nonlinear dynamics of the plant that are unknown. It is assumed that if X is a bounded state vector, then $\alpha_k(t)$ and $\beta_k(t)$ are bounded signals. Throughout the analysis to follow, both $\alpha_k(t)$ and $\beta_k(t)$ may be set to zero for all $t \geqslant 0$.

Definition 1. The dynamics for a relative degree r plant described by 2.1 (as shown in Spooner and Passino (1996)) may be written in normal form as

$$\dot{\xi}_1 = \xi_2, \tag{2.4}$$

$$\vdots \quad \vdots \tag{2.5}$$

$$\dot{\xi}_{r-1} = \xi_r, \tag{2.6}$$

$$\dot{\xi}_r = \alpha(\xi, \pi) + \beta(\xi, \pi)u_p, \tag{2.7}$$

$$\dot{\pi} = \Psi(\xi, \pi) \tag{2.8}$$

with $\pi \in \Re^{n-r}$, and $y_p = \xi_1$. The "zero-dynamics" of the system are given as

$$\dot{\pi} = \Psi(0, \pi). \tag{2.9}$$

Here, we will consider plants that either have no zero dynamics (i.e., $n = r$), or plants with zero dynamics (i.e., $1 \leqslant r < n$) that are exponentially attractive. These types of plants are defined in the following plant assumptions (Spooner and Passino, 1996).

2.2. Plant assumptions

Assumption 1. The plant is of relative degree $r = n$ (i.e. no zero dynamics), such that

$$\frac{\mathrm{d}}{\mathrm{d}t} x_i = x_{i+1}, \quad i = 1, \ldots, n-1,$$

$$\frac{\mathrm{d}}{\mathrm{d}t} x_n = \alpha(X) + \alpha_k(t) + (\beta(X) + \beta_k(t))u_p,$$

where $y_p = x_1$, with $\alpha_k(t)$ and $\beta_k(t)$ known functions. Here it is assumed that there exists $\beta_0 > 0$ such that $\beta(X) + \beta_k(t) \geqslant \beta_0$, and that $x_1, \ldots, x_n$ are measurable.

Assumption 2. The plant is of relative degree r, $1 \leqslant r < n$, with the zero dynamics exponentially attractive and there exists $\beta_0 > 0$ such that $\beta(X) + \beta_k(t) \geqslant \beta_0$. The outputs $y_p, \ldots, y_p^{(r-1)}$ are measurable.

It is clear that plants satisfying Assumption 1 have bounded states if the reference input and its derivatives are bounded, and the output error and its derivatives are also bounded. It can also be shown (as in Spooner and Passino (1996)) that plants satisfying Assumption 2 have bounded states if the output is bounded.

Next, a brief description of direct and indirect adaptive control schemes will be presented.

2.3. Direct adaptive control

A direct adaptive controller, that seeks to drive the output of a relative degree r plant y_p to track a known desired output trajectory y_m, uses an approximator that attempts to approximate the ideal controller dynamics (u^*, that we assume to exist) by adjusting the controller

parameters. Hence, our objective is design a controller which makes the output of the plant y_p track the output trajectory y_m. In additions to the plant Assumptions 1 and 2, we use the following plant assumption (Spooner and Passino, 1996).

Assumption 3. Given $y_p^{(r)} = (\alpha(X) + \alpha_k(t)) + (\beta(X) + \beta_k(t))u_p$, we require that $\beta_k(t) = 0$, $t \geqslant 0$, and that there exists positive constants β_0 and β_1 such that $0 < \beta_0 \leqslant \beta(X) \leqslant \beta_1 < \infty$ and some function $B(X) \geqslant 0$ such that $|\dot{\beta}(X)| = |(\partial\beta/\partial X)\dot{X}| \leqslant B(X)$ for all $X \in S_x$. Here, $\alpha_k(t)$ is a known time dependent signal. Here, we also require the following output trajectory assumption (Spooner and Passino, 1996).

Assumption 4. The desired output trajectory and its derivatives $y_m, \ldots, y_m^{(r)}$ are measurable and bounded.

Using feedback linearization (Sastry and Bodson, 1989), we know that there exists some ideal controller

$$u^* = \frac{1}{\beta(X)}(-\alpha(X) + v(t)), \tag{2.10}$$

where $v(t) \coloneqq y_m^{(r)} + \delta e_s + \bar{e}_s - \alpha_k(t)$, with $\bar{e}_s \coloneqq \dot{e}_s - e_o^{(r)}$, and $\delta > 0$. For now we assume that $\beta_k(t) + \hat{\beta}(X)$ is bounded away from zero so that (2.10) is well-defined, however, we shall later show how to ensure that this is the case. The tracking error is defined as $e_s \coloneqq k^{\mathrm{T}} e$ where $e \coloneqq [e_o, \dot{e}_o, \ldots, e_o^{(r-1)}]^{\mathrm{T}}$, $k \coloneqq [k_0, \ldots, k_{r-2}, 1]^{\mathrm{T}}$, and $e_o \coloneqq y_m - y_p$, thus $\bar{e}_s = [\dot{e}_o, \ldots, e_o^{(r-1)}][k_0, \ldots, k_{r-2}]^{\mathrm{T}}$. We pick the elements of k such that $L(s) \coloneqq s^{r-1} + k_{r-2}s^{r-2} + \cdots + k_1 s + k_0$ has its roots in the open left half plane. The goal of the adaptive controller is to "learn" how to control the plant to drive e_s (which is a measure of the tracking error) to some neighborhood of zero. We may express u^* as

$$u^* = A_u^{*\top}\zeta_u(X, v) + u_k + d_u(X). \tag{2.11}$$

The ideal parameter vector, A_u^*, is defined as

$$A_u^* \coloneqq \arg \min_{A_u \in \Omega_u} \left[\sup_{X \in S_x, v \in S_m} |A_u^{\top}\zeta_u(X, v) - (u^* - u_k)| \right], \tag{2.12}$$

where A_u is assumed to be defined within the compact parameter set Ω_u, and S_x and $S_m \subseteq \Re^n$ are defined as the spaces through which the state trajectory and the free parameter $v(t)$ may travel under closed-loop control. Also, ζ_u is defined as the partial of the approximator with respect to the parameter vector, u_k is a known part of the controller, and $d_u(X)$ is the approximation error which arises when u^* is represented by an approximator (e.g., fuzzy system, neural network, or other universal approximator) of finite size. It is assumed that $|d_u(X)| \leqslant D_u(X)$, where $D_u(X)$ is a known upper bound on the error. Since universal approximators are used for approximation, $|d_u(x)|$ may be made arbitrarily small by a proper choice of the approximator structure. To do this, we will require X and v to be available. The ideal control (2.10) can be approximated by

$$u_d = A_u^{\top}\zeta_u + u_k, \tag{2.13}$$

where A_u is updated on line. Using the control (2.13), the rth derivative of the output error becomes

$$e_o^{(r)} = y_m^{(r)} - y_p^{(r)} = y_m^{(r)} - \alpha(X) - \alpha_k(t) - \beta(X)u_d. \tag{2.14}$$

Using the definition of u^* (2.10) we may rearrange (2.14) so that

$$e_o^{(r)} = y_m^{(r)} - \alpha(X) - \alpha_k(t) - \beta(X)u^* - \beta(X)(u_d - u^*) \tag{2.15}$$

$$= -\delta e_s - \bar{e}_s - \beta(X)(u_d - u^*). \tag{2.16}$$

We may alternatively express (2.16) as

$$\dot{e}_s + \delta e_s = -\beta(X)(u_d - u^*). \tag{2.17}$$

Assume for now that parameter vector, $A_u(k)$, is updated on line using a hybrid adaptive law (in later section, we will discuss this adaptive law in detail). Define the approximator parameter error as $\phi(k) = A_u(k) - A_u^*$. Using the definitions of the ideal control (2.11) and the actual one (2.13), it can be shown that

$$u_d - u^* = \phi(k)^{\top}\zeta_u - d_u(X). \tag{2.18}$$

Substituting (2.18) into (2.17), we can define $\hat{e} \coloneqq u^* - u_d$ in the direct case such that

$$\hat{e} = \frac{\dot{e}_s + \delta e_s}{\beta(X)} = -\phi(k)^{\top}\zeta_u + d_u(X). \tag{2.19}$$

Note that $\hat{e}$ (which is a function of the plant dynamics, $\beta(X)$) is a measure of the tracking performance, and will be used in the parameter hybrid update law (as we will show in later sections).

2.4. Indirect adaptive control

Unlike the direct approach, in the indirect approach we approximate the plant dynamics ($\alpha(x)$ and $\beta(x)$), then the feedback controller uses these estimates of the plant dynamics to tune the parameters of the controller so that the plant output y_p tracks the output trajectory y_m. The plant dynamics $\alpha(X)$ and $\beta(X)$ can be expressed as

$$\alpha(X) = A_\alpha^{*\top}\zeta_\alpha(X) + d_\alpha(X), \tag{2.20}$$

$$\beta(X) = A_\beta^{*\top}\zeta_\beta(X) + d_\beta(X), \tag{2.21}$$

where

$$A_\alpha^* \coloneqq \arg \min_{A_\alpha \in \Omega_\alpha} \left[\sup_{X \in S_x} |A_\alpha^{\top}\zeta_\alpha(X) - \alpha(X)| \right], \tag{2.22}$$

$$A_\beta^* \coloneqq \arg \min_{A_\alpha \in \Omega_\beta} \left[\sup_{X \in S_x} |A_\beta^{\top}\zeta_\beta(X) - \beta(X)| \right]. \tag{2.23}$$

The parameter vectors, A_α and A_β, are assumed to be defined within the compact parameter sets, Ω_α and Ω_β,

respectively. In addition, we define the subspace $S_x \subseteq \Re^n$ as the space through which the state trajectory may travel under closed-loop control. Also, $d_\alpha(X)$ and $d_\beta(X)$ are approximation errors which arise when $\alpha(X)$ and $\beta(X)$ are represented by approximators of finite size. We assume that $D_\alpha(X) \geqslant |d_\alpha(X)|$, and $D_\beta(X) \geqslant |d_\beta(X)|$, where $D_\alpha(X)$ and $D_\beta(X)$ are known bounds on the approximation errors. Since universal approximators (e.g., fuzzy systems, neural networks, and others (Wang, 1994)), both $|d_\alpha(X)|$ and $|d_\beta(X)|$ may be made arbitrarily small by a proper choice of the approximator if $\alpha(X)$ and $\beta(X)$ are smooth. It is important to keep in mind that $D_\alpha(X)$ and $D_\beta(X)$ represent the magnitude of error between the actual nonlinear functions describing the system dynamics and the approximators when the "best" parameters are used.

We assume that the actual plant dynamics, $\alpha(X)$ and $\beta(X)$, can be expressed as

$$\hat{\alpha}(X) = A_\alpha^\top \zeta_\alpha, \tag{2.24}$$

$$\hat{\beta}(X) = A_\beta^\top \zeta_\beta, \tag{2.25}$$

where the vectors $A_\alpha(k)$ and $A_\beta(k)$ are updated on line (as we will show later) using a hybrid adaptive law. The parameter error vectors

$$\phi_\alpha(k) = A_\alpha(k) - A_\alpha^*, \tag{2.26}$$

$$\phi_\beta(k) = A_\beta(k) - A_\beta^*, \tag{2.27}$$

are used to define the difference between the current estimate of the parameters (at time k) and the best values of the parameters defined by (2.22) and (2.23). The certainty equivalence control term (Sastry and Isidori, 1989) is defined as

$$u_i = \frac{1}{\beta_k(t) + \hat{\beta}(X)}[-(\alpha_k(t) + \hat{\alpha}(X)) + v(t)], \tag{2.28}$$

where $v(t) \coloneqq y_m^{(r)} + \delta e_s + \bar{e}_s$, with e_s and $\bar{e}_s$ defined as in the direct case. For now we assume that $\beta_k(t) + \hat{\beta}(X)$ is bounded away from zero so that (2.28) is well-defined, however, we shall later show how to ensure that this is the case. Using the control (2.28), the rth derivative of the output error becomes $e_o^{(r)} = y_m^{(r)} - y_p^{(r)}$ so

$$e_o^{(r)} = y_m^{(r)} - (\alpha_k(t) + \alpha(X)) - \frac{\beta_k(t) + \beta(X)}{\beta_k(t) + \hat{\beta}(X)} \times [-(\alpha_k(t) + \hat{\alpha}(X)) + v(t)]. \tag{2.29}$$

We may rearrange terms so that

$$e_o^{(r)} = \left[1 - \frac{\beta_k(t) + \beta(X)}{\beta_k(t) + \hat{\beta}(X)}\right](-(\alpha_k(t) + \hat{\alpha}(X)) + v(t)) - \alpha(X) + \hat{\alpha}(X) - \delta e_s - \bar{e}_s \tag{2.30}$$

$$= (\hat{\alpha}(X) - \alpha(X)) + (\hat{\beta}(X) - \beta(X))u_i - \delta e_s - \bar{e}_s. \tag{2.31}$$

We may express (2.31) as

$$\dot{e}_s + \delta e_s = (\hat{\alpha}(X) - \alpha(X)) + (\hat{\beta}(X) - \beta(X))u_i. \tag{2.32}$$

Analogous to the direct case, it can be shown that

$$\hat{\alpha}(X) - \alpha(X) = \phi_\alpha^\top \zeta_\alpha - d_\alpha(X), \tag{2.33}$$

$$\hat{\beta}(X) - \beta(X) = \phi_\beta^\top \zeta_\beta - d_\beta(X). \tag{2.34}$$

Substituting (2.33) and (2.34) in (2.32), we get

$$\dot{e}_s + \delta e_s = \left[\phi_\alpha^\top \zeta_\alpha - d_\alpha(X)\right] + \left[\phi_\beta^\top \zeta_\beta - d_\beta(X)\right]u_i = \phi^\top \zeta - [d_\alpha(X) + d_\beta(X)], \tag{2.35}$$

where $\phi = \left[\phi_\alpha^\top, \phi_\beta^\top\right]^\top$, and $\zeta = \left[\zeta_\alpha^\top, \zeta_\beta^\top u_i\right]^\top$. Let us define $\hat{e}$ as

$$\hat{e} \coloneqq -\dot{e}_s - \delta e_s = -\phi^\top \zeta + [d_\alpha(X) + d_\beta(X)]. \tag{2.36}$$

Note that $\hat{e}$ is a measure of the tracking performance, and will be used in the parameter hybrid update law (as we will show in later sections).

In summary, the measure of tracking performance $\hat{e}$ for both direct and indirect cases can be written as

$$\hat{e} \coloneqq \frac{\kappa(\dot{e}_s + \delta e_s)}{\theta(X)} = -\phi^\top \zeta + d, \tag{2.37}$$

where the parameters for both direct and indirect cases are summarized in the Table 1.

Next, we present a hybrid adaptive law that can be used for parameter adaptation.

3. Hybrid adaptive law: update and stability

Consider the adaptive law

$$\dot{A} = \eta \varepsilon \zeta, \tag{3.1}$$

where the $\dot{A}$ is the derivative of the parameter vector with respect to time, $\eta > 0$ is a scalar adaptation gain, and $\varepsilon \coloneqq \hat{e}/m^2$. As defined in Ioannou and Sun (1996), $m^2 = 1 + n_s^2$, and m is designed so that ζ/m and

Table 1
Summary of parameters

	κ	$\theta(X)$	d	$\phi(t)$	$\zeta(t)$
Direct	1	$\beta(X)$	$d_u(X)$	$\phi_u(t)$	$\zeta_u(t)$
Indirect	-1	1	$d_\alpha(X) + d_\beta(X)$	$\left[\phi_\alpha(t)^\top, \phi_\beta(t)^\top\right]^\top$	$\left[\zeta_\alpha(t)^\top, \zeta_\beta(t)^\top u_i(t)\right]^\top$

$d(X)/m \in \mathscr{L}_\infty$, and n_s is chosen such that $|\zeta|/m \leqslant 1$. A typical choice for n_s^2 is $n_s^2 = \gamma\zeta^\top\zeta$, where $\gamma \geqslant 1$. The adaptive law (3.1) is usually used with systems that have no modeling error (Ioannou and Sun, 1996). In the presence of modeling error, however, a *leakage* modification is often used. The idea behind leakage is to modify the adaptive law (3.1) so that the time derivative of the Lyapunov function used to analyze the adaptive scheme becomes negative in the space of the parameter estimates when these parameters exceed certain bounds (Ioannou and Sun, 1996). One way to solve this problem is to modify the adaptive law (3.1) as follows:

$$\dot{A} = \eta\varepsilon\zeta - w\eta A, \tag{3.2}$$

where w (which will be defined later) is a positive scalar signal (i.e., $w(t) \geqslant 0$) that is designed so that stability is maintained if the parameter error exceeds a certain bound.

In the update law (3.2), the parameter vector A is updated continuously with time, such that at every instant of time, t, we have a new estimate of the parameter vector. In many cases, it is desirable to update the estimate at specific instants of time t_k, where $\{t_k\}$ is an unbounded monotonically increasing sequence in $\mathscr{R}^+$. Let $t_k = kT_s$ where $T_s = t_{k+1} - t_k$ is the sampling period, and $k \in \mathscr{N}^+$ (i.e., $k = 0, 1, \ldots$). To derive the hybrid adaptive law, integrate the continuous adaptive law (3.2) from some time instant $t_k = kT_s$ to the subsequent time instant $t_{k+1} = (k+1)T_s$ to have

$$A(k+1) = A(k) + \eta \int_{t_k}^{t_{k+1}} [\varepsilon(\tau)\zeta(\tau) - w(\tau)A(k)]\,\mathrm{d}\tau, \tag{3.3}$$

where $A(k) \coloneqq A(t_k)$. Note that the adaptive law (3.3) generates a sequence of estimates $A(k) = A(kT_s)$, for $k = 0, 1, 2, \ldots$. Although $\varepsilon(t)$ and $\zeta(t)$ may change over time, the estimate $A(k)$ is constant for $t \in [t_k, t_{k+1})$. As mentioned earlier, stability and boundedness results that can be obtained using the hybrid adaptive law (3.3) is dependent on the choice of the parameter $w(t)$. In Ioannou and Sun (1996), some stability results have been established for the "switching σ-modification". The choice of $w(t)$ in the switching σ-modification is defined as $w(t) = \sigma_s$, where

$$\sigma_s = \begin{cases} 0 & \text{if } |A(k)| < M_0, \\ \sigma_0 & \text{if } |A(k)| \geqslant M_0 \end{cases} \tag{3.4}$$

$\sigma_0 > 0$, and $M_0 \geqslant 2|A^*|$. Note that the adaptive law (3.2) has actually been analyzed in Ioannou and Sun (1996) for three different choices of the leakage term $w(t)$. These choices are the σ-modification, the switching-σ modification, and the ε-modification. The authors in Ioannou and Sun (1996) have shown that, unlike the σ-modification and the ε-modification, the switching-σ modification is able to achieve robustness without having to destroy some important properties (i.e., ε, εm, $\dot{A} \in \mathscr{L}_2$) of the adaptive law. Also, the selection of a discontinuous σ_s (3.4) fits the discrete-time nature of the adaptive law (3.3). For a more detailed analysis on the choices of $w(t)$ refer to Ioannou and Sun (1996).

Next, we will show the stability properties that are established by the hybrid adaptive law (3.3). However, before we start the theorem, let us state the following definition.

Definition 2. Let $x : [0, \infty) \to \mathscr{R}^n$, where $x \in \mathscr{L}_{2e}$ (the $\mathscr{L}_{2e}$ norm is defined as $\|x(t)\|_2 \coloneqq (\int_0^{\mathrm{T}} |x(\tau)|^2\,\mathrm{d}\tau)^{1/2}$, and we say that $x(t) \in \mathscr{L}_{2e}$ when $\|x(t)\|_2$ exists for any finite t), and consider the set

$$\mathscr{S}(\mu) = \left\{ x : [0,\infty) \to \mathscr{R}^n \middle| \int_t^{t+T_s} x^\top(\tau)x(\tau)d(\tau) \leqslant c_0\mu T_s + c_1,\ \forall t,\ T_s \geqslant 0 \right\} \tag{3.5}$$

for a given constant $\mu \geqslant 0$, where $c_0, c_1 \geqslant 0$ are some finite constants, and c_0 is independent of μ. If $x \in \mathscr{S}$, we say that x is μ-small in the mean square sense.

Theorem 1. *Let m, σ_0, T_s, η be chosen so that*

- $\frac{d}{m} \in \mathscr{L}_\infty$, $\frac{\zeta^\top\zeta}{m^2} \leqslant 1$,
- $2T_s\eta < 1$, $2\sigma_0 T_s\eta < 1$.

Then the hybrid adaptive law (3.3) *guarantees that*

(1) ε, $\varepsilon n_s \in \mathscr{L}_\infty$, $A(k) \in l_\infty$ (*for a sequence $x = (x_1, x_2, \ldots)$ and $x_i \in \mathscr{R}$ where $i \geqslant 1$, the l_∞ norm is defined as $\|x\|_\infty \coloneqq \sup_{i\geqslant 1}|x_i|$. We say that $x \in l_\infty$ if $\|x\|_\infty$ exists*).
(2) ε, $\varepsilon m \in \mathscr{S}(d^2/m^2)$.

Proof. This proof follows the one in Ioannou and Sun (1996) but with appropriate modifications for the theory. □

Now, we will state the stability results for continuous-time direct and indirect adaptive control schemes when the hybrid adaptive law is used.

Theorem 2. *Given the error dynamics* (2.37) *with the reference trajectory assumption* (*Assumption* 4) *satisfied, and either Assumption* 1 *or* 2 *holds* (*and for the direct case, Assumption* 3 *holds*), *then the hybrid adaptive law in both direct and indirect cases will ensure* (*in addition to the results stated in Theorem* 1) *that*

1. *e_s is bounded.*
2. *The plant output and its derivatives $y_p, \ldots, y_p^{(r-1)}$ are bounded.*
3. *The control signal* (u_d *in the direct case or* u_i *in the indirect case*) *is bounded.*

The proof can be found in the Appendix.

4. Auto-tuning the adaptation gain

In this section, we will present a methodology to auto-tune the adaptation gain for a continuous-time nonlinear adaptive control systems when a gradient-based hybrid adaptive law is used for parameter adaptation. The gradient update law relies on the following idea. Starting with an initial value for the parameter vector, the gradient algorithm changes (updates) this vector by adding to it another vector having a magnitude and a direction of descent. We can think of this as searching for the ideal parameter vector. In most adaptive schemes, the adaptation gain is held constant. Here, however, we argue that the adaptation gain can be selected (adapted) on-line to minimize the instantaneous control energy. It is important to mention that our objective here is to search for an "optimal" η (that we will call η^{opt}). Note that η^{opt} is not necessarily the optimal adaptation gain. The step of finding η^{opt} is crucial to find the new parameter vector ($A^{\text{opt}}(k)$), and hence the new control, $u^{\text{opt}}(t)$. The term *optimal* is used here only because the adaptation gain (as shown below) will be selected to minimize the instantaneous control energy $J_u(\eta) = u^2(t)$. We would like to note that the adaptation gain $\eta(k)$ is fixed over the interval $[t_k, t_{k+1})$.

4.1. Auto-tuning algorithm

The adaptation gain tuning algorithm (for both direct and indirect adaptive cases) proceeds according to the following steps (shown in Fig. 1):

1. Find a range on $\eta(k)$ (i.e., $\eta \in [\eta_{\min}, \eta_{\max}]$), such that the stability is maintained no matter which $\eta(k)$ in this range is used.
2. Find the new adaptation gain ($\eta^{\text{opt}}(k)$) that minimizes the instantaneous control energy $J_u(\eta) = u^2(t)$.
3. Using $\eta^{\text{opt}}(k)$, find the new parameter vector $A^{\text{opt}}(k)$ and hence the new control $u^{\text{opt}}(t)$.

4.1.1. Finding a feasible range on $\eta(k)$

Recall from Theorem 1 that the parameters m, σ_0, T_s, $\eta(k)$ need to be chosen so that

$$2T_s\eta(k) < 1 \tag{4.1}$$

or

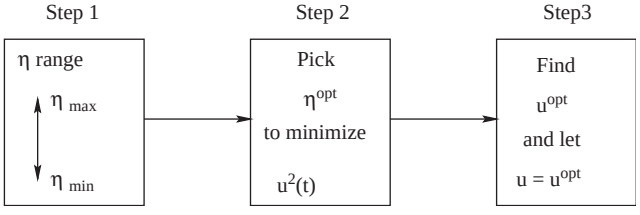

Fig. 1. Steps used for adaptation gain selection.

$$\eta(k) < \frac{1}{2T_s} \tag{4.2}$$

and

$$2\sigma_0 T_s \eta(k) < 1 \tag{4.3}$$

or

$$\eta(k) < \frac{1}{2\sigma_0 T_s}. \tag{4.4}$$

To satisfy both conditions (4.2) and (4.4), we select $\eta(k)$ such that

$$\eta(k) < \min\left\{\frac{1}{2T_s}, \frac{1}{2\sigma_0 T_s}\right\} \coloneqq \bar{\eta}, \tag{4.5}$$

where $\bar{\eta}$ is an upper bound on the adaptation gain. Define $\eta(k) = \rho(k)\bar{\eta}$ and

$$[\eta_{\min} = \rho_1\bar{\eta}] \leqslant [\eta(k) = \rho(k)\bar{\eta}] [\leqslant \rho_2\bar{\eta} = \eta_{\max}], \tag{4.6}$$

where $0 < \rho_1 \leqslant \rho(k) \leqslant \rho_2 < 1$ for fixed constants ρ_1 and ρ_2. Note that both $\eta(k)$ and $\rho(k)$ are constants over the interval $[t_k, t_{k+1})$.

4.1.2. Finding the new adaptation gain $\eta^{\text{opt}}(k)$ via minimizing the instantaneous control energy

Here, the new adaptation gain is obtained by minimizing the following cost function

$$\min J_u(\eta) = u^2(t) \tag{4.7}$$

such that $\eta_{\min} \leqslant \eta(k) \leqslant \eta_{\max}$. Assume that the ideal control can be approximated by

$$u(t) = A^{\top}(k)\zeta(t), \tag{4.8}$$

where $A(k)$ is constant over the interval $[t_k, t_{k+1})$. Substituting the hybrid adaptive law (3.3) into (4.8), we get

$$\begin{aligned} u(t) &= \left[A(k-1) + \eta(k)\int_{t_{k-1}}^{t_k} [\varepsilon(\tau)\zeta(\tau) - w(\tau) \right. \\ &\quad \left. \times A(k-1)]\,\mathrm{d}\tau\right]^{\top}\zeta(t) \\ &= A(k-1)^{\top}\zeta(t) + \eta(k) \\ &\quad \times \left[\int_{t_{k-1}}^{t_k} [\varepsilon(\tau)\zeta(\tau) - w(\tau)A(k-1)]\,\mathrm{d}\tau\right]^{\top}\zeta(t). \end{aligned} \tag{4.9}$$

Let $\varphi_1(t) = [\int_{t_{k-1}}^{t_k} [\varepsilon(\tau)\zeta(\tau) - w(\tau)A(k-1)]\,\mathrm{d}\tau]^{\top}\zeta(t)$ and $\varphi_2(t) = A(k-1)^{\top}\zeta(t)$, then $u(t)$ can be written as $u(t) = \varphi_1(t)\eta(k) + \varphi_2(t)$. Hence, $u^2(t)$ can be written as $u^2(t) = \varphi_1^2(t)\eta^2(k) + 2\varphi_1(t)\varphi_2(t)\eta(k) + \varphi_2^2(t)$. Since $u^2(t)$ is in quadratic form, the cost function (4.7) can be minimized as a quadratic programming problem with linear inequality constraint ($\eta_{\min} \leqslant \eta(k) \leqslant \eta_{\max}$). Since $\varphi_2^2(t)$ is independent of $\eta(k)$, it can be omitted from the cost function we want to minimize. Hence, the instantaneous control energy $u^2(t)$ (that we need to minimize to obtain

the new adaptation gain) can be expressed as

$$\min_\eta u^2(t) = \min_\eta \ \varphi_1^2(t)\eta^2(k) + 2\varphi_1(t)\varphi_2(t)\eta(k)$$
$$\text{s.t. } \eta_{\min} \leqslant \eta(k) \leqslant \eta_{\max}. \tag{4.10}$$

Since $\varphi_1^2(t)$ is positive definite, this problem (4.10) is known to have a unique global minimum, $\eta^{\text{opt}}(k)$, which can be used to find the new parameter vector and hence the new control. Now, this adaptation gain can be used in the update routine of the controller's parameter vector as shown next.

4.1.3. Finding the new parameter vector ($A^{\text{opt}}(k)$) and the new control ($u^{\text{opt}}(t)$)

The new adaptation gain $\eta^{\text{opt}}(k)$ can be used to find the new parameter vector $A^{\text{opt}}(k)$ as follows:

$$A^{\text{opt}}(k) = A^{\text{opt}}(k-1) + \eta^{\text{opt}}(k) \times \int_{t_{k-1}}^{t_k} [\varepsilon(\tau)\zeta(\tau) - w(\tau)A^{\text{opt}}(k-1)]\,\mathrm{d}\tau. \tag{4.11}$$

This new parameter vector of the controller is used to find the new control as

$$u^{\text{opt}}(t) = A^{\text{opt}\top}(k)\zeta(t), \tag{4.12}$$

which is the final control to be input to the system.

4.2. Stability analysis

Here, we will present the stability results when the adaptation gain is auto-tuned according to the algorithm presented above.

Theorem 3. *Let m, σ_0, T_s, $\eta(k)$ be chosen so that $d/m \in \mathscr{L}_\infty$, $\zeta^\top\zeta/m^2 \leqslant 1$, then the hybrid adaptive law* (4.11) (*when the adaptation gain is auto-tuned to minimize the instantaneous control energy*) *guarantees that*

(1) ε, $\varepsilon n_s \in \mathscr{L}_\infty$, $A(k) \in l_\infty$,
(2) ε, $\varepsilon m \in \mathscr{S}(\frac{d^2}{m^2})$.

The proof can be found in the Appendix A. Now, we present the following theorem to show boundedness of all signals.

Theorem 4. *Given the error dynamics* (2.37) *with the reference trajectory assumption* (*Assumption* 4) *satisfied, and either Assumption* 1 *or* 2 *holds* (*and for the direct case, Assumption* 3 *holds*), *then the hybrid adaptive law* (4.11) *in both direct and indirect cases will ensure* (*in addition to the results stated in Theorem* 3) *that*

1. *e_s is bounded.*
2. *The plant output and its derivatives $y_p, \ldots, y_p^{(r-1)}$ are bounded.*
3. *The control signal (u_d in the direct case or u_i in the indirect case) is bounded.*

Proof. The proof of this theorem is similar to the proof of Theorem 2. □

5. Aircraft wing rock example

Aircraft wing rock is a limit cycling oscillation in the aircraft roll angle ϕ and roll rate $\dot\phi$. Limit cycle roll and roll rate are experienced by aircraft with pointed forebodies at high angle of attack. Such phenomenon may present serious danger due to the potential of aircraft instability. If δ_A is the actuator output, a model of this phenomenon is given by

$$\ddot\phi = a_1\phi + a_2\dot\phi + a_3\dot\phi^3 + a_4\phi^2\dot\phi + a_5\phi\dot\phi^2 + b\delta_A. \tag{5.1}$$

Choose the state vector $x = [x_1, x_2, x_3]^\top$ with $x_1 = \phi$, $x_2 = p = \dot\phi$, and $x_3 = \delta_A$. Suppose that we use a first order model to represent the actuator dynamics of the aileron (the control surface at the outer part of the wing). Then we have

$$\begin{aligned}
\dot x_1 &= x_2,\\
\dot x_2 &= a_1x_1 + a_2x_2 + a_3x_2^3 + a_4x_1^2x_2 + a_5x_1x_2^2 + bx_3,\\
\dot x_3 &= -\frac{1}{\tau}x_3 + \frac{1}{\tau}u,\\
y &= x_1,
\end{aligned} \tag{5.2}$$

where u is the control input to the actuator and τ is the aileron time constant. For an angle of attack of 21.5°, $a_1 = -0.0148927$, $a_2 = 0.0415424$, $a_3 = 0.01668756$, $a_4 = -0.06578382$, and $a_5 = 0.08578836$. Also, $b = 1.5$ and $\tau = \frac{1}{15}$. Here, we use an initial condition of $x(0) = [0.4, 0, 0]^\top$. Here, the reference signal $y_m(t) = 0$. The above model was taken from Nayfeh et al. (1989) and Elzebda et al. (1989) and is based on wind tunnel data in Levin and Katz (1984). The objective of this example is to demonstrate the auto-tuning algorithm presented earlier.

Based on the definition of the plant considered (2.1) we can show that

$$f(X) = \begin{bmatrix} x_2 \\ a_1x_1 + a_2x_2 + a_3x_2^3 + a_4x_1^2x_2 + a_5x_1x_2^2 + bx_3 \\ -\frac{1}{\tau}x_3 \end{bmatrix}, \tag{5.3}$$

$$g(X) = \begin{bmatrix} 0 \\ 0 \\ \frac{1}{\tau} \end{bmatrix} \tag{5.4}$$

and

$$h(X) = x_1. \tag{5.5}$$

Also, it can be verified that the relative degree of the system is $r = n = 3$ (no zero dynamics). It can be shown (according to (2.3)) that

$$y^{(3)} = (\alpha_k(t) + \alpha(X)) + (\beta_k(t) + \beta(X))u, \tag{5.6}$$

where (assuming that $\alpha_k(t) = \beta_k(t) = 0$)

$$\alpha(X) = a_1x_2 + 2a_4x_1x_2^2 + a_5x_2^3 - \frac{b}{\tau}x_3 + [a_2 + 3a_3x_2^2 + a_4x_1^2 + 2a_5x_1x_2] \times [a_1x_1 + a_2x_2 + a_3x_2^3 + a_4x_1^2x_2 + a_5x_1x_2^2 + bx_3] \quad (5.7)$$

and

$$\beta(X) = \frac{b}{\tau}. \quad (5.8)$$

Here, it is assumed that there exists positive constants β_0 and β_1 such that $0 < \beta_0 \leqslant \beta(X) \leqslant \beta_1 < \infty$, where in this case $\beta_0 = 10$ and $\beta_1 = 40$.

As defined earlier, our measure of the tracking performance is

$$\varepsilon = \frac{\kappa(\dot{e}_s + \delta e_s)}{\theta(X)m^2}, \quad (5.9)$$

where $e_s = k^{\top}e$ and $k = [k_0, k_1, 1] = [100, 20, 1]$.

5.1. Direct case

Here, we attempt to approximate the ideal controller by an approximator in the form of a Takagi–Sugeno fuzzy system (TSFS). The TSFS used here has nine rules, and it has two inputs to the premise of each rule, x_1 and x_2. Also, it has three inputs to the consequent of each rule, x_1, x_2, and x_3. The certainties of the rules are determined by Gaussian membership functions whose centers are evenly distributed between -2 and 2. The parameters of the TSFS are updated using the hybrid adaptive law

$$A(k) = A(k-1) + \eta(k) \times \int_{t_{k-1}}^{t_k} [\varepsilon(\tau)\zeta(\tau) - w(\tau)A^{\text{opt}}(k-1)]\,\mathrm{d}\tau. \quad (5.10)$$

After some tuning, we have found that we can obtain a small value of ε (as shown in Fig. 2) using $T_s = 0.005$, $\sigma_0 = 1$, $M_0 = 1$, $\gamma = 1.8$, and $\delta = 30$. The value of T_s is chosen to be 0.005 since small sampling time is needed to simulate such a continuous time system. To simplify the tuning procedure, σ_0 is chosen to be 1 so that

$$\frac{1}{2T_s} = \frac{1}{2\sigma_0 T_s}$$

and hence $\bar{\eta}$ defined in (4.5) becomes

$$\bar{\eta} = \min\left\{\frac{1}{2T_s} = \frac{1}{2\sigma_0 T_s}\right\} = \frac{1}{2T_s} = \frac{1}{2\sigma_0 T_s}.$$

Based on theory, γ should be selected such that $\gamma \geqslant 1$. Here, we started with $\gamma = 1$, and we found by some tuning that an acceptable response can be achieved using $\gamma = 1.8$. Also, δ which needs to be positive serves as a weighting between e_s and $\dot{e}_s$ in the definition of ε. We started with $\delta = 1$. After some tuning, we have found that $\delta = 30$ is an acceptable choice. Based on the

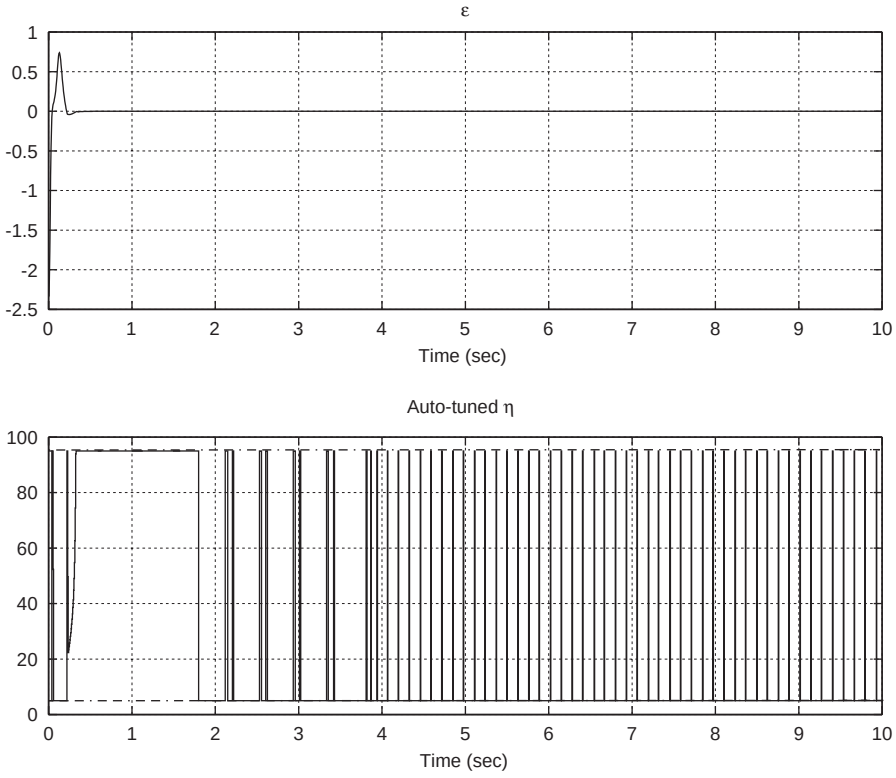

Fig. 2. The responses of ε and η in the direct case.

theory, M_0 has to be selected such that $M_0 \geqslant 2|A^*|$. Since $|A^*|$ is unknown, we initially selected M_0 to be some large positive scalar, and by some tuning we were able to decrease the magnitude of this scalar to $M_0 = 1$ such that we achieve some acceptable performance. Using (4.5), it can be easily shown that $\bar{\eta} = 100$. Here, we selected ρ_1 and ρ_2 to be 0.05 and 0.95, respectively. This implies that the lower and upper bounds on the adaptation gain are 5 and 95, respectively. In the fist plot of Fig. 2, we show how ε decreases to a small value. The second plot in the figure shows how the adaptation gain varies based on the variations of ε. It is clear from the figure that the adaptation gain, in almost the first 2 s, increases to its upper bound since large adaptation gain is needed to derive ε to some small value. After the 2 s, the adaptation gain usually takes its lower bound since ε has small value over that time. However, at certain instants the adaptation gain starts to increase to its upper bound for relatively short time intervals. It is unclear from Fig. 2 why the adaptation gain behaves in such mannerafter the first two seconds (when ε is relatively small). To investigate this observation, we consider Fig. 3, where the first plot which is a scaled version of the first plot in Fig. 2 shows the behavior of ε at a smaller range. It is clear from this figure that ε exhibits small variations in magnitude. This shows (for this particular example) how sensitive the presented auto-tuning algorithm is for small variations in ε. It is important to note that since $\varepsilon \in \mathscr{S}(d^2/m^2)$, ε can be made smaller by either decreasing d^2 (by improving the approximation accuracy) or by increasing m^2 (by increasing γ). The response of the aircraft roll angle, ϕ, is shown in the first plot of Fig. 4. The second plot of this figure shows the behavior of the aileron input, δ_A. It is clear that the response of the aircraft roll angle is unacceptable with this set of controller parameters. However, such results are expected since the objective of the adaptive control law is to drive ε (not the tracking error, e_0) to a small value that is function of d and m (since $\varepsilon \in \mathscr{S}(d^2/m^2)$). We know that ε is defined as

$$\varepsilon = \frac{\kappa(\dot{e}_s + \delta e_s)}{\theta(X)m^2} \in \mathscr{S}\left(\frac{d^2}{m^2}\right).$$

One way to decrease the tracking error is to try to make e_s dominate the effects on the dynamics of ε (by increasing the value of δ), and hence e_0 will become smaller since e_s is smaller. This is clear from the response of the aircraft roll angle shown in Fig. 5 when δ is increased to 5000. Note that the algorithm presented earlier focuses on auto-tuning the adaptation gain by minimizing the control energy. For this reason, let us discuss how this algorithm impacts the resulting control energy. To do that, we need to investigate how the MSE and MCE change for different values over the feasible range of adaptation gain (which is in this case $0 < \eta < 100$). Fig. 6 shows how both the MCE and MSE change for several fixed values of the adaptation

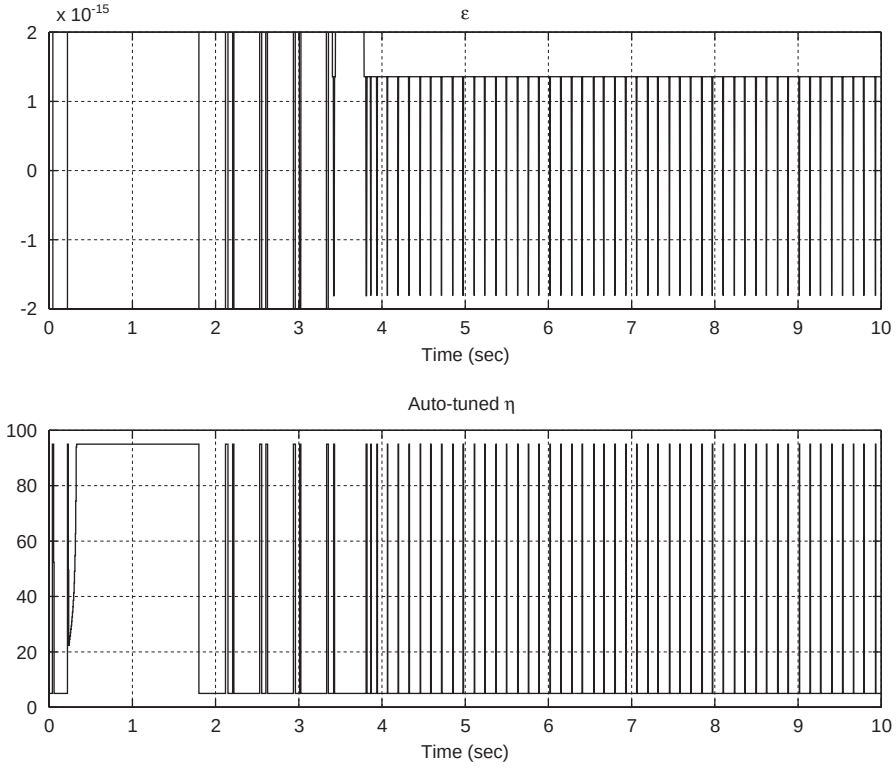

Fig. 3. The responses of ε and η in the direct case.

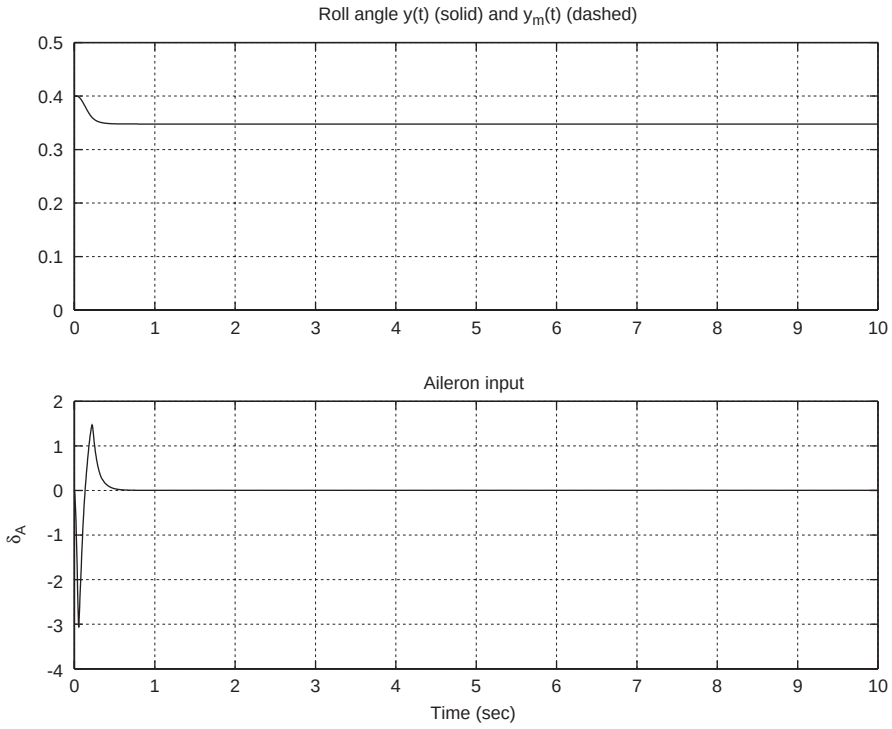

Fig. 4. The responses of the aircraft roll angle and aileron input in the direct case for $\delta = 30$.

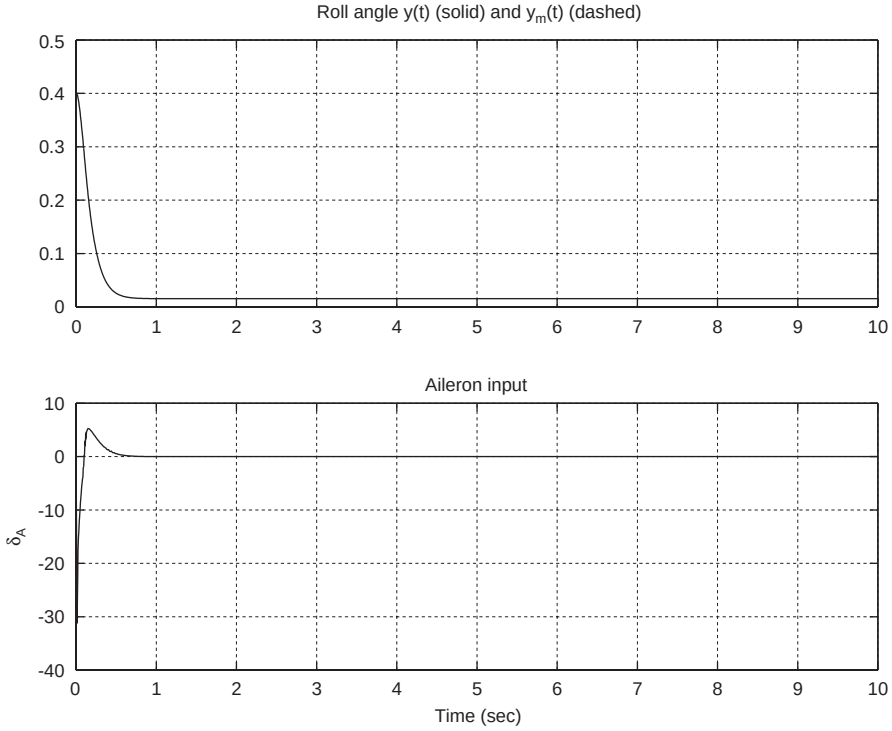

Fig. 5. The responses of the aircraft roll angle and aileron input in the direct case for $\delta = 5000$.

gain over a simulation period of 10 s. The first plot in Fig. 6 shows the changes in MCE for several values of the adaptation gain. The dotted line in this figure shows the value of the MCE when the auto-tuning algorithm is used. This value is found to be 0.2205. It is clear that MCE (except at very small values of η) slightly oscillates

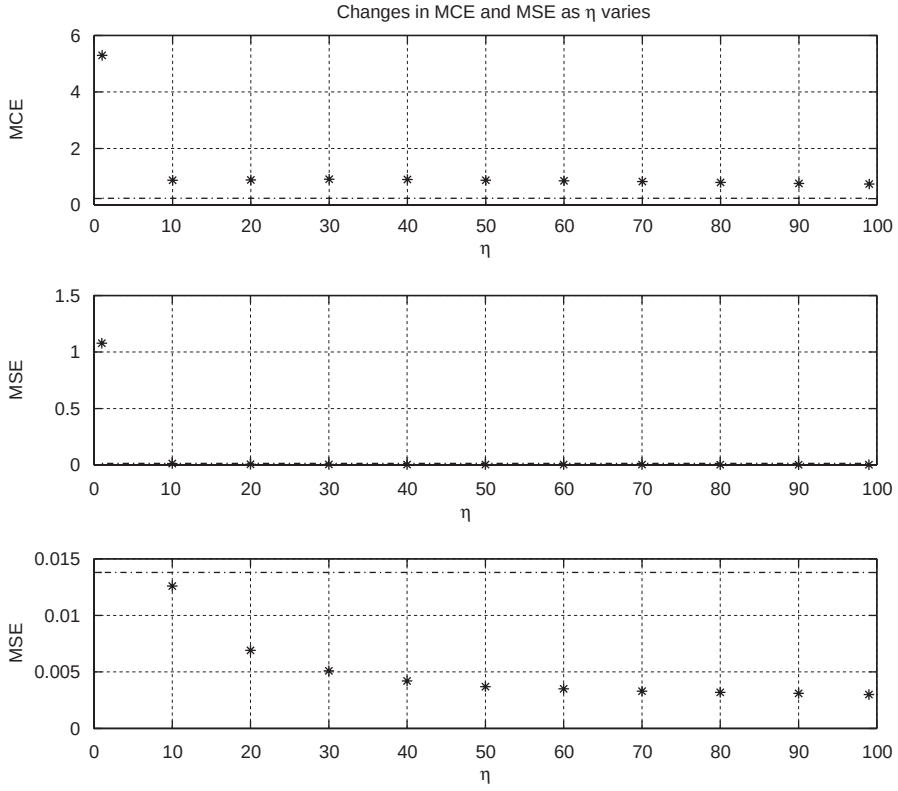

Fig. 6. Changes in the MCE and MSE as η varies in the direct adaptive case.

around 0.9. The large MCE values at small fixed values of η can be due to the large error that may result when small fixed values of η are used. To decrease such large error, a relatively large control energy is often needed. It is clear that the MCE achieved when the auto-tuning algorithm is used is smaller than the MCE obtained using any fixed adaptation gain. Similarly, the second plot in the figure shows the changes in MSE for several fixed values of the adaptation gain, and the dotted line shows the value of the MSE when the auto-tuning algorithm is used. This value is found to be 0.0138. The third plot is only a scaled version of the second plot to clarify the variation of MSE at large values of the adaptation gain. It is clear from the figure that the MSE decreases as the adaptation gain increases. This decrease is due to the relatively large control energy (compared to the MCE obtained using the auto-tuning algorithm) that improves the closed-loop performance. The MSE obtained using the auto-tuning algorithm is found to be larger than almost any MSE value obtained at a fixed adaptation gain. This is due to the fact that in the auto-tuning algorithm the adaptation gain is obtained to minimize the control energy at the expense of error energy. Hence, we can conclude that our simulation results support the objective of the presented algorithm in the sense that the adaptation gain is selected on-line to minimize the control energy in such a way that a good closed-loop performance is achieved.

5.2. Indirect case

Here, we attempt to approximate parts of the plant dynamics (i.e., $\alpha(X)$ and $\beta(X)$) and use these estimates to find the control. The function α is approximated here by an approximator in the form of a Takagi–Sugeno fuzzy system (TSFS) that has nine rules. This TSFS has two inputs to the premise of each rule, x_1 and x_2. Also, it has three inputs to the consequent of each rule, x_1, x_2, and x_3. The certainties of the rules are determined by Gaussian membership functions whose centers are evenly distributed between -2 and 2. The function $\beta(X)$, however, is approximated by a scalar. The parameters of both approximators are updated using the hybrid adaptive law (5.10). After some tuning, we have found that we can obtain a small value of ε (as shown in Fig. 7) using $T_s = 0.005$, $\sigma_0 = 1$, $M_0 = 200$, $\gamma = 3$, and $\delta = 3$. T_s and σ_0 are chosen to be 0.005 and 1, respectively, for the same reason stated in the direct case. Also, since γ should be selected such that $\gamma \geqslant 1$, we started with $\gamma = 1$, and we found by some tuning that good response can be achieved using $\gamma = 3$. As in the direct case, δ needs to be positive; we started with $\delta = 1$, and after some tuning we have found that $\delta = 3$ is an acceptable choice. Also, M_0 has to be selected such that $M_0 \geqslant 2|A^*|$. Since $|A^*|$ is unknown, we initially M_0 to be some large positive scalar, and by some tuning we have found that $M_0 = 200$ provides an acceptable

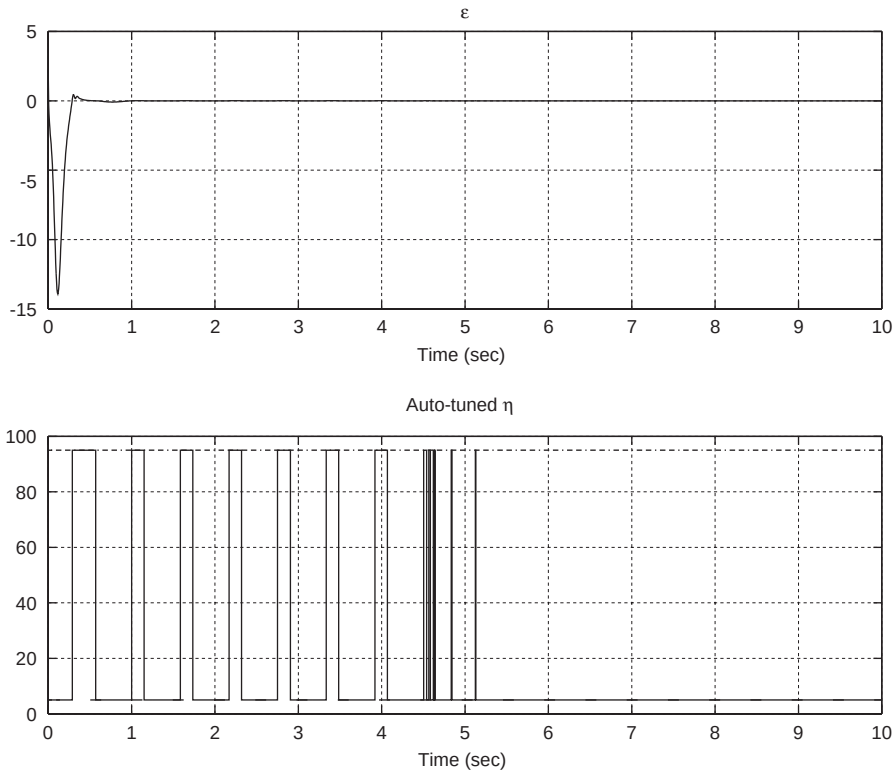

Fig. 7. The responses of ε and η in the indirect case.

performance. Using (4.5), it can be easily shown that $\bar{\eta} = 100$. Here, we selected ρ_1 and ρ_2 to be 0.05 and 0.95, respectively. This implies that the lower and upper bounds on the adaptation gain are 5 and 95, respectively. The responses of ε and η are shown in Fig. 7. In the first plot of Fig. 7, we show how ε decreases to a small value. The second plot in the figure shows how the adaptation gain varies based on the variations of ε. It is clear from the figure that the adaptation gain, in almost the first 5 s, increases to its upper bound whenever necessary to keep ε small, and after that the adaptation gain decreases to its lower bound since ε is small enough that no major changes in the approximators are needed and hence small adaptation gain is sufficient. As in the direct case, $\varepsilon \in \mathscr{S}(d^2/m^2)$, ε can be made smaller by either decreasing d^2 or by increasing m^2. The response of the aircraft roll angle, ϕ, is shown in the first plot of Fig. 8. The second plot of this figure shows the behavior of the aileron input, δ_A. It is clear that the response of the aircraft roll angle is unacceptable with this set of controller parameters. As in the direct case, however, such results are expected since the objective of the adaptive control law is to drive ε (not the tracking error, e_0) to a small value. The main difference is that δ cannot be made much larger than what we have here (we can only increase it to about 20), and hence e_s (and e_0) cannot be driven to smaller values. The response of the aircraft roll angle and aileron input in the for $\delta = 20$ is shown in Fig. 9. As in the direct case, we need to investigate how the MSE and MCE change for different values over the feasible range of adaptation gain (which is in this case $0 < \eta < 100$). Fig. 10 shows how both the MCE and MSE change for several fixed values of the adaptation gain over a simulation period of 10 s. The first plot in Fig. 10 shows the changes in MCE for several values of the adaptation gain. The dotted line in this figure shows the value of the MCE when the auto-tuning algorithm is used. This value is found to be 0.2074. It is clear that MCE (except at very small values of η) slightly oscillate around 0.9. The reason behind large MCE values at small fixed values of η is stated earlier in the direct case. It is clear that the MCE achieved when the auto-tuning algorithm is used is larger than most MCE values obtained using fixed adaptation gains. Similarly, the second plot in the figure shows the changes in MSE for several fixed values of the adaptation gain, and the dotted line shows the value of the MSE when the auto-tuning algorithm is used. This value is found to be 1.6528. The third plot is only a scaled version of the second plot to clarify the variation of MSE at large values of the adaptation gain. It is clear from the figure that the MSE decreases as the adaptation gain increases. This decrease is due to the relatively large control energy (compared to the MCE obtained using the auto-tuning algorithm) that improves the closed-loop performance. The MSE obtained using the auto-tuning algorithm is found to be larger than almost any MSE value obtained at a fixed adaptation

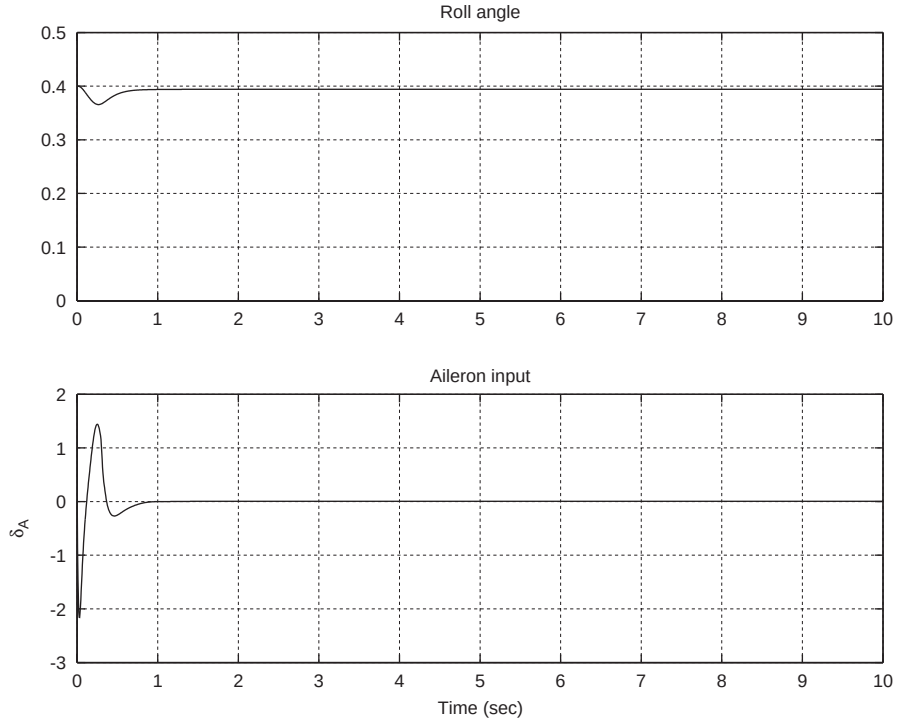

Fig. 8. The responses of the aircraft roll angle and aileron input in the indirect case for $\delta = 3$.

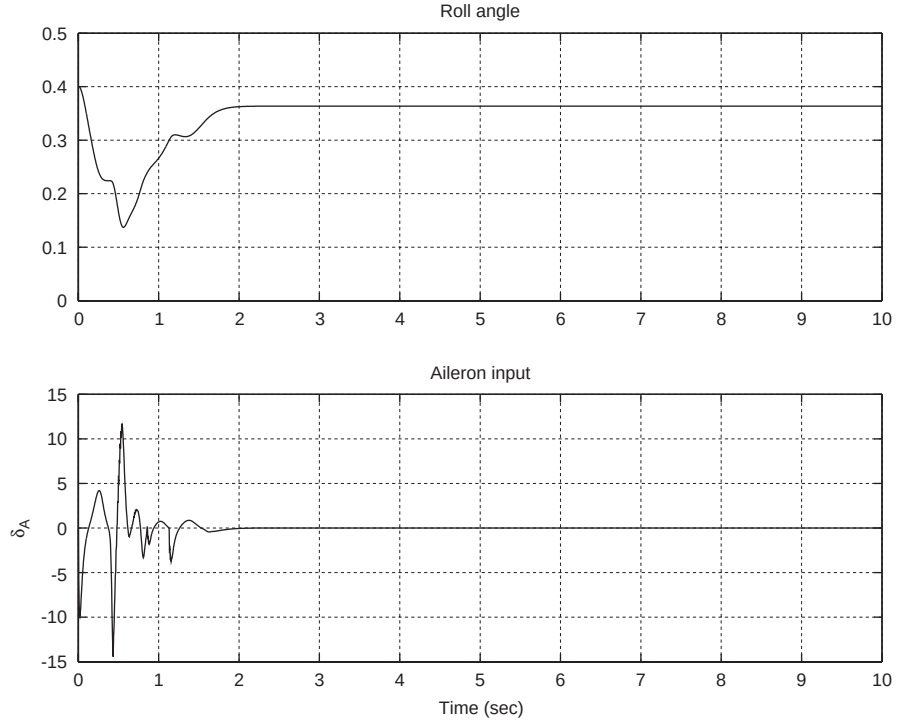

Fig. 9. The responses of the aircraft roll angle and aileron input in the indirect case for $\delta = 20$.

gain. As in the direct case, this is due to the fact that in the auto-tuning algorithm the adaptation gain is obtained to minimize the control energy at the expense of error energy. Hence, we can also conclude that our simulation results support the objective of the presented algorithm in the sense that the adaptation gain is selected on-line to minimize the control energy in such a way that a good closed-loop performance is achieved.

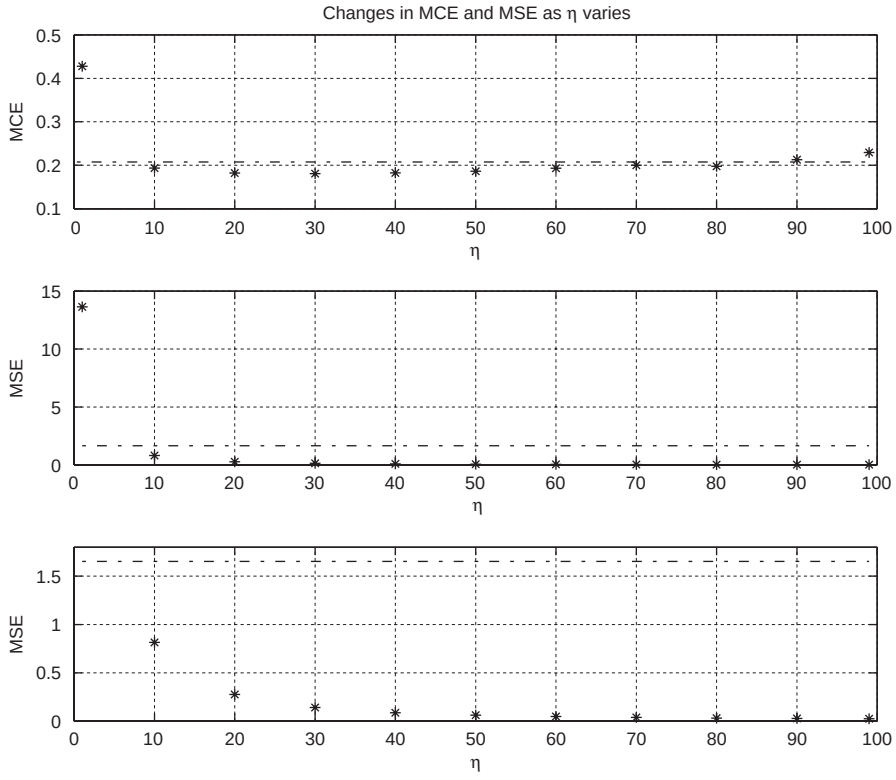

Fig. 10. Changes in the MCE and MSE as η varies in the indirect adaptive case.

6. Conclusion

Considering both direct and indirect adaptive control schemes, the main contribution of this paper is to auto-tune the adaptation gain for a gradient-based approximator parameter update law used for a class of continuous-time nonlinear systems. The adaptation mechanism of the gradient update law is usually based on minimizing the squared output error. Here, however, we auto-tune the adaptation gain to minimize the control energy. Based on the simulation results of the wing rock example, a comparison to some extent can be made between direct and indirect adaptive control schemes. Unlike the direct case, it is shown by the example that in the indirect case it is not feasible to decrease e_s (and hence the tracking error, e_0) to small values.

Appendix A

A.1. Proof of Theorem 2

Part 1: From Theorem 1 we know that

$$\varepsilon = \frac{\kappa(\dot{e}_s + \delta e_s)}{\theta m^2} \in \mathscr{S}\left(\frac{d^2}{m^2}\right). \tag{A.1}$$

Rearranging terms, (A.1) can be written as

$$\dot{e}_s + \delta e_s = \frac{\varepsilon\theta m^2}{\kappa}. \tag{A.2}$$

The differential equation shown in (A.2) is a first order non-homogeneous differential equation, and its solution can be written as the sum of the homogeneous solution and the particular one (i.e., $e_s = (e_s)_{\mathrm{h}} + (e_s)_{\mathrm{p}}$, where $(e_s)_{\mathrm{h}}$ and $(e_s)_{\mathrm{p}}$ are the homogeneous and particular solutions, respectively). It can be shown that the homogeneous solution has the form

$$(e_s)_{\mathrm{h}} = c_e \mathrm{e}^{-\delta t}, \tag{A.3}$$

where c_e is a constant that depends on the initial condition, and the particular solution is

$$(e_s)_{\mathrm{p}} = \frac{\varepsilon\theta m^2}{\kappa\delta}. \tag{A.4}$$

Hence, e_s can be expressed as

$$e_s = c_e \mathrm{e}^{-\delta t} + \frac{\varepsilon\theta m^2}{\kappa\delta}. \tag{A.5}$$

Since $\delta > 0$, $c_e \mathrm{e}^{-\delta t}$ decreases exponentially as time increases. Hence

$$\lim_{t\to\infty} e_s = \frac{\varepsilon\theta m^2}{\kappa\delta}. \tag{A.6}$$

We know from Theorem 1 that both of ε and $\varepsilon m \in \mathscr{S}(d^2/m^2)$. This implies that m is bounded. Since all parameters in the right-hand side of (A.6) are bounded, e_s is bounded.

Part 2: Hence, $|e_s|$ is bounded by some upper bound $M_e(d,m)$ (i.e., $|e_s| \leqslant M_e$). The following analysis, to show that the output error and its derivatives are bounded provided that $|e_s| \leqslant M_e$, has been discussed in Spooner and Passino (1996). Define transfer functions

$$\hat{G}_i(s) \coloneqq \frac{s^i}{\hat{L}(s)}, \quad i = 0, \ldots, r-1, \tag{A.7}$$

which are stable since $\hat{L}(s)$ has its poles in the open left half plane. Since $e_o^{(i)} = \hat{G}_i(s) e_s$, with e_s bounded, then $e_o^{(i)}$ is bounded (i.e., $e_o^{(i)} \in \mathscr{L}_\infty$). Since $e_o^{(i)}$ is bounded and $e_o^{(i)} = y_m^{(i)} - y_p^{(i)}$, and $y_m^{(i)}$ is bounded (by Assumption 4), then the output and its derivatives are bounded ($y_p^{(i)} \in \mathscr{L}_\infty$, $\forall i = 0, 1, ..., r-1$). This establishes the second part of the theorem.

Part 3: Since the output and its derivatives are bounded, using Assumptions 1 or 2 we know that the states of the plant are bounded. Hence, in the indirect case the functions $\alpha(X)$, $\alpha_k(t)$, $\beta(X)$, $\beta_k(t) \in \mathscr{L}_\infty$. The projection algorithm, ensures that $\beta_k(t) + \hat{\beta}(X)$ is bounded away from zero and that $\hat{\alpha}(X)$ is bounded, thus $u_i \in \mathscr{L}_\infty$. In the direct case, since the states are bounded then ζ is bounded. Also, we can use a projection algorithm to ensure that $A \in \mathscr{L}_\infty$. Hence, from the definition of the control u_d (2.13), we know that u_d is bounded (i.e., $u_d \in \mathscr{L}_\infty$). This establishes the third part of the theorem. □

A.2. Proof of Theorem 3

Consider the following Lyapunov-like function

$$V(k) = \phi(k)^\top \phi(k). \tag{A.8}$$

Since $A(k+1) - A^* = A(k) - A^* + A(k+1) - A(k)$, we know that

$$\phi(k+1) = \phi(k) + \Delta A(k), \tag{A.9}$$

where

$$\Delta A(k) = \rho(k+1)\bar{\eta} \int_{t_k}^{t_{k+1}} [\varepsilon(\tau)\zeta(\tau) - w(\tau)A(k)]\,\mathrm{d}\tau. \tag{A.10}$$

Here, $\rho(k)\bar{\eta} = \eta(k)$ represents any adaptation gain within the feasible range

$$[\eta_{\min} = \rho_1\bar{\eta}] \leqslant [\eta(k) = \rho(k)\bar{\eta}] \leqslant [\eta_{\max} = \rho_2\bar{\eta}],$$

where $0 < \rho_1 \leqslant \rho \leqslant \rho_2 < 1$. Using (A.9) in (A.8), we can write

$$\begin{aligned} V(k+1) &= [\phi(k) + \Delta A(k)]^\top [\phi(k) + \Delta A(k)] \\ &= \phi(k)^\top \phi(k) + 2\phi(k)^\top \Delta A(k) + \Delta A^\top(k)\Delta A(k) \\ &= V(k) + 2\phi(k)^\top \Delta A(k) + \Delta A^\top(k)\Delta A(k). \end{aligned} \tag{A.11}$$

Substituting (A.10) in (A.11), we get

$$\begin{aligned} V(k+1) = V(k) &+ 2\phi(k)^\top \rho(k+1)\bar{\eta} \\ &\times \int_{t_k}^{t_{k+1}} [\varepsilon(\tau)\zeta(\tau) - w(\tau)A(k)]\,\mathrm{d}\tau \\ &+ \int_{t_k}^{t_{k+1}} [\varepsilon(\tau)\zeta(\tau) - w(\tau)A(k)]^\top \mathrm{d}\tau \\ &\times [\rho(k+1)\bar{\eta}]^2 \\ &\times \int_{t_k}^{t_{k+1}} [\varepsilon(\tau)\zeta(\tau) - w(\tau)A(k)]\,\mathrm{d}\tau. \end{aligned} \tag{A.12}$$

Using (2.37) and the definition that $\varepsilon = \hat{e}/m^2$, it can be easily shown that

$$\phi(k)^\top \zeta = -\varepsilon m^2 + d \tag{A.13}$$

or

$$\phi(k)^\top \varepsilon\zeta = -\varepsilon^2 m^2 + \varepsilon d. \tag{A.14}$$

Integrating both sides of (A.14), we get

$$\begin{aligned} &\phi(k)^\top \int_{t_k}^{t_{k+1}} \varepsilon(\tau)\zeta(\tau)\,\mathrm{d}\tau \\ &\quad = \int_{t_k}^{t_{k+1}} [-\varepsilon^2(\tau)m^2(\tau) + \varepsilon(\tau)\,\mathrm{d}(\tau)]\,\mathrm{d}\tau. \end{aligned} \tag{A.15}$$

We know that $-a^2 + ab \leqslant -(a^2/2) + (b^2/2)$. Let $a = \varepsilon m$ and $b = d/m$. Hence, (A.15) can be written as

$$\begin{aligned} \phi(k)^\top \int_{t_k}^{t_{k+1}} \varepsilon(\tau)\zeta(\tau)\,\mathrm{d}\tau \leqslant &- \int_{t_k}^{t_{k+1}} \frac{\varepsilon^2(\tau)m^2(\tau)}{2}\,\mathrm{d}\tau \\ &+ \int_{t_k}^{t_{k+1}} \frac{d^2(\tau)}{2m^2(\tau)}\,\mathrm{d}\tau. \end{aligned} \tag{A.16}$$

Consider the last term in (A.12) and note that

$$\begin{aligned} &\int_{t_k}^{t_{k+1}} [\varepsilon(\tau)\zeta(\tau) - w(\tau)A(k)]^\top \mathrm{d}\tau [\rho(k+1)\bar{\eta}]^2 \\ &\quad \times \int_{t_k}^{t_{k+1}} [\varepsilon(\tau)\zeta(\tau) - w(\tau)A(k)]\,\mathrm{d}\tau \\ &\qquad = [\rho(k+1)\bar{\eta}]^2 \left| \int_{t_k}^{t_{k+1}} [\varepsilon(\tau)\zeta(\tau) - w(\tau)A(k)]\,\mathrm{d}\tau \right|^2. \end{aligned} \tag{A.17}$$

Since $(a+b)^2 \leqslant 2a^2 + 2b^2$, where $a = \int_{t_k}^{t_{k+1}} \varepsilon(\tau)\zeta(\tau)\,d\tau$ and $b = \int_{t_k}^{t_{k+1}} -w(\tau)A(k)\,d\tau$, then

$$\left|\int_{t_k}^{t_{k+1}} [\varepsilon(\tau)\zeta(\tau) - w(\tau)A(k)]\,d\tau\right|^2 \leqslant 2\left|\int_{t_k}^{t_{k+1}} \varepsilon(\tau)m(\tau)\frac{\zeta(\tau)}{m(\tau)}\,d\tau\right|^2 + 2\left|\int_{t_k}^{t_{k+1}} w(\tau)A(k)\,d\tau\right|^2. \quad (A.18)$$

Also, since $|\zeta(t)|/m(t) \leqslant 1$, $w(t) \leqslant \sigma_s^2$, and $\int_{t_k}^{t_{k+1}} |A(k)|^2\,d\tau = |A(k)|^2 T_s^2$, then

$$2\left|\int_{t_k}^{t_{k+1}} \varepsilon(\tau)m(\tau)\frac{\zeta(\tau)}{m(\tau)}\,d\tau\right|^2 + 2\left|\int_{t_k}^{t_{k+1}} w(\tau)A(k)\,d\tau\right|^2 \leqslant 2T_s\int_{t_k}^{t_{k+1}} \varepsilon^2(\tau)m^2(\tau)\,d\tau + 2\sigma_s^2 T_s^2|A(k)|^2. \quad (A.19)$$

Hence, from (A.17) to (A.19), we can say that

$$\int_{t_k}^{t_{k+1}} [\varepsilon(\tau)\zeta(\tau) - w(\tau)A(k)]^\top\,d\tau[\rho(k+1)\bar{\eta}]^2 \times \int_{t_k}^{t_{k+1}} [\varepsilon(\tau)\zeta(\tau) - w(\tau)A(k)]\,d\tau \leqslant 2[\rho(k+1)\bar{\eta}]^2 T_s\int_{t_k}^{t_{k+1}} \varepsilon^2(\tau)m^2(\tau)\,d\tau + 2[\rho(k+1)\bar{\eta}]^2\sigma_s^2 T_s^2|A(k)|^2. \quad (A.20)$$

It can be shown that (A.12) can be written as

$$V(k+1) \leqslant V(k) + 2\rho(k+1)\bar{\eta}\phi^\top(k)\int_{t_k}^{t_{k+1}} \varepsilon(\tau)\zeta(\tau)\,d\tau + \int_{t_k}^{t_{k+1}} [\varepsilon(\tau)\zeta(\tau) - w(\tau)A(k)]^\top\,d\tau[\rho(k+1)\bar{\eta}]^2 \times \int_{t_k}^{t_{k+1}} [\varepsilon(\tau)\zeta(\tau) - w(\tau)A(k)]\,d\tau - 2\rho(k+1)\bar{\eta}\phi^\top(k)\int_{t_k}^{t_{k+1}} w(\tau)A(k)\,d\tau. \quad (A.21)$$

Using (A.16) and (A.20) in (A.21), we have

$$V(k+1) \leqslant V(k) - \rho(k+1)\bar{\eta}\int_{t_k}^{t_{k+1}} \varepsilon^2(\tau)m^2(\tau)\,d\tau + \rho(k+1)\bar{\eta}\int_{t_k}^{t_{k+1}} \frac{d^2(\tau)}{m^2(\tau)}\,d\tau - 2\rho(k+1)\bar{\eta}\sigma_s T_s\phi(k)^\top A(k) + 2[\rho(k+1)\bar{\eta}]^2 T_s\int_{t_k}^{t_{k+1}} \varepsilon^2(\tau)m^2(\tau)\,d\tau + 2[\rho(k+1)\bar{\eta}]^2\sigma_s^2 T_s^2|A(k)|^2. \quad (A.22)$$

Rearranging terms, (A.22) becomes

$$V(k+1) \leqslant V(k) - \rho(k+1)\bar{\eta}[1 - 2\rho(k+1)\bar{\eta}T_s] \times \int_{t_k}^{t_{k+1}} \varepsilon^2(\tau)m^2(\tau)\,d\tau + \rho(k+1)\bar{\eta}\int_{t_k}^{t_{k+1}} \frac{d^2(\tau)}{m^2(\tau)}\,d\tau - 2\rho(k+1)\bar{\eta}\sigma_s T_s\left[\phi(k)^\top A(k) - \rho(k+1)\bar{\eta}\sigma_s T_s|A(k)|^2\right]. \quad (A.23)$$

Using the fact that $|A^*| \geqslant |A(k)|$, we know that

$$\begin{aligned}\phi(k)^\top A(k) &= [A(k) - A^*]^\top A(k)\\ &= |A(k)|^2 - A^{*\top}A(k)\\ &\geqslant |A(k)|^2 - |A^*||A(k)|\\ &\geqslant |A(k)|^2 - |A^*|^2\\ &\geqslant \frac{|A(k)|^2}{2} - \frac{|A^*|^2}{2}.\end{aligned} \quad (A.24)$$

Using (A.24) in (A.23), we have

$$V(k+1) \leqslant V(k) - \rho(k+1)\bar{\eta}[1 - 2\rho(k+1)\bar{\eta}T_s] \times \int_{t_k}^{t_{k+1}} \varepsilon^2(\tau)m^2(\tau)\,d\tau + \rho(k+1)\bar{\eta}\int_{t_k}^{t_{k+1}} \frac{d^2(\tau)}{m^2(\tau)}\,d\tau - 2\rho(k+1)\bar{\eta}\sigma_s T_s\left[\frac{|A(k)|^2}{2} - \frac{|A^*|^2}{2} - \rho(k+1)\bar{\eta}\sigma_s T_s|A(k)|^2\right] \quad (A.25)$$

or

$$V(k+1) \leqslant V(k) - \rho(k+1)\bar{\eta}[1 - 2\rho(k+1)\bar{\eta}T_s] \times \int_{t_k}^{t_{k+1}} \varepsilon^2(\tau)m^2(\tau)\,d\tau + \rho(k+1)\bar{\eta}\int_{t_k}^{t_{k+1}} \frac{d^2(\tau)}{m^2(\tau)}\,d\tau - 2\rho(k+1)\bar{\eta}\sigma_s T_s\left[\left(\frac{1}{2} - \rho(k+1)\bar{\eta}\sigma_0 T_s\right) \times |A(k)|^2 - \frac{|A^*|^2}{2}\right]. \quad (A.26)$$

Let $D_m = \sup_t d/m \in \mathscr{L}_\infty$. Since D_m is constant over the time $[t_k, t_{k+1})$, then (A.26) becomes

$$V(k+1) \leqslant V(k) - \rho(k+1)\bar{\eta}[1 - 2\rho(k+1)\bar{\eta}T_s] \times \int_{t_k}^{t_{k+1}} \varepsilon^2(\tau)m^2(\tau)\,d\tau + T_s\rho(k+1)\bar{\eta}|D_m|^2 - 2\rho(k+1)\bar{\eta}\sigma_s T_s\left[\left(\frac{1}{2} - \rho(k+1)\bar{\eta}\sigma_0 T_s\right) \times |A(k)|^2 - \frac{|A^*|^2}{2}\right]. \quad (A.27)$$

From the definition (4.5), we know that

$$\rho(k+1)\bar{\eta} < \bar{\eta} \leqslant \frac{1}{2T_s} \tag{A.28}$$

and

$$\rho(k+1)\bar{\eta} < \bar{\eta} \leqslant \frac{1}{2\sigma_0 T_s}. \tag{A.29}$$

From (A.28) and (A.29), we know that

$$2\rho(k+1)\bar{\eta}T_s < 1 \tag{A.30}$$

and

$$\rho(k+1)\bar{\eta}\sigma_0 T_s < \tfrac{1}{2}. \tag{A.31}$$

To show that $A(k) \in l_\infty$, we need to consider two cases: the case when $|A(k)| < M_0$ and the case when $|A(k)| \geqslant M_0$. In the first case (when $|A(k)| < M_0$ for some bounded parameter M_0), it clear that $A(k) \in l_\infty$. In the other case (when $|A(k)| \geqslant M_0$ and hence $\sigma_s = \sigma_0$), however, we consider (A.27). In (A.27) (when (A.30) and (A.31) are both satisfied), we can guarantee that $V(k+1) \leqslant V(k)$ whenever

$$T_s\rho(k+1)\bar{\eta}|D_m|^2 - 2\sigma_s T_s\rho(k+1)\bar{\eta}\left[\tfrac{1}{2} - \rho(k+1)\bar{\eta}\sigma_0 T_s\right] |A(k)|^2 + \rho(k+1)\bar{\eta}\sigma_s T_s|A^*|^2 \leqslant 0 \tag{A.32}$$

or since $\sigma_s = \sigma_0$

$$|A(k)|^2 \geqslant \frac{|D_m|^2 + \sigma_0|A^*|^2}{\sigma_0[1 - 2\rho(k+1)\bar{\eta}\sigma_0 T_s]}. \tag{A.33}$$

Since in this case we know that $|A(k)| \geqslant M_0$, we can guarantee that $V(k+1) \leqslant V(k)$ whenever

$$|A(k)|^2 \geqslant \max\left\{ M_0^2, \frac{|D_m|^2 + \sigma_0|A^*|^2}{\sigma_0[1 - 2\eta\sigma_0 T_s]} \right\}. \tag{A.34}$$

Note, here, that M_0 is assumed to be large enough (e.g., $M_0 \geqslant 1$) such that $M_0 \geqslant |A^*|$. We can conclude from (A.34) (since all of its parameters are bounded) that $V(k+1) \leqslant V(k)$. Since $V(k)$ is defined as $V(k) = \phi(k)^\top \phi(k)$, then it can be shown (for some bounded parameter initial condition, $A(0) \in l_\infty$) that $A(k) \in l_\infty$. Since all parameters in the hybrid adaptive law (4.11) are bounded, then we can conclude that ε and hence εm are bounded. This establishes the first part of the theorem.

To establish the second part, consider

$$\begin{aligned}
&\sigma_s\phi^\top(k)A(k) \\
&\quad = \sigma_s A(k)^\top A(k) - \sigma_s A^{*\top} A(k) \\
&\quad = \frac{\sigma_s}{2} A(k)^\top A(k) + \left[\frac{\sigma_s}{2} A(k)^\top A(k) - \sigma_s A^{*\top} A(k)\right] \\
&\quad \geqslant \frac{\sigma_s}{2}|A(k)|^2 + \frac{\sigma_s}{2}\left[|A(k)|^2 - 2|A^*||A(k)|\right] \\
&\quad \geqslant \frac{\sigma_s}{2}|A(k)|^2 + \frac{\sigma_s}{2}|A(k)|[|A(k)| - 2|A^*|].
\end{aligned} \tag{A.35}$$

Since $M_0 \geqslant 2|A^*|$, (A.35) becomes

$$\sigma_s\phi^\top(k)A(k) \geqslant \frac{\sigma_s}{2}|A(k)|^2 + \frac{\sigma_s}{2}|A(k)|[|A(k)| - M_0]. \tag{A.36}$$

Also, using (3.4) in (A.36), we get

$$\sigma_s\phi^\top(k)A(k) \geqslant \frac{\sigma_s}{2}|A(k)|^2. \tag{A.37}$$

Adding and subtracting $\sigma_0\rho(k+1)\bar{\eta}T_s$ from the right-hand side of (A.37), and using the fact that $2\sigma_0\rho(k+1)\bar{\eta}T_s < 1$, (A.37) becomes

$$\sigma_s\phi^\top(k)A(k) \geqslant \sigma_s\left[\tfrac{1}{2} + \rho(k+1)\bar{\eta}\sigma_0 T_s - \rho(k+1)\bar{\eta}\sigma_0 T_s\right]|A(k)|^2. \tag{A.38}$$

Defining $c_\sigma = \frac{1}{2} - \rho(k+1)\bar{\eta}\sigma_0 T_s$, (A.38) can be written as

$$\sigma_s\left[\phi^\top(k)A(k) - \rho(k+1)\bar{\eta}\sigma_0 T_s|A(k)|^2\right] \geqslant \sigma_s c_\sigma |A(k)|^2. \tag{A.39}$$

Rearranging terms, (A.23) can be written as

$$\begin{aligned}
&\rho(k+1)\bar{\eta}[1 - 2\rho(k+1)\bar{\eta}T_s]\int_{t_k}^{t_{k+1}} \varepsilon^2(\tau)m^2(\tau)\,\mathrm{d}\tau \\
&\quad + 2\rho(k+1)\bar{\eta}\sigma_s T_s\left[\phi(k)^\top A(k) - \rho(k+1)\bar{\eta}\sigma_s T_s|A(k)|^2\right] \\
&\qquad \leqslant V(k) - V(k+1) + \rho(k+1)\bar{\eta}\int_{t_k}^{t_{k+1}} \frac{d^2(\tau)}{m^2(\tau)}\,\mathrm{d}\tau
\end{aligned} \tag{A.40}$$

and using (A.39), (A.40) becomes

$$\begin{aligned}
&\rho(k+1)\bar{\eta}[1 - 2\rho(k+1)\bar{\eta}T_s]\int_{t_k}^{t_{k+1}} \varepsilon^2(\tau)m^2(\tau)\,\mathrm{d}\tau \\
&\quad + 2\rho(k+1)\bar{\eta}\sigma_s T_s c_\sigma |A(k)|^2 \\
&\qquad \leqslant V(k) - V(k+1) + \rho(k+1)\bar{\eta}\int_{t_k}^{t_{k+1}} \frac{d^2(\tau)}{m^2(\tau)}\,\mathrm{d}\tau
\end{aligned} \tag{A.41}$$

which implies that $\varepsilon m \in \mathscr{S}(d^2/m^2)$. Since $|\varepsilon| \leqslant |\varepsilon m|$ (because $m \geqslant 1$), we conclude that $\varepsilon \in \mathscr{S}(d^2/m^2)$. □

References

Chen, F.-C., Khalil, H.K., 1995. Adaptive control of a class of nonlinear discrete-time systems using neural networks. IEEE Transactions on Automatic Control 40, 791–801.

Elzebda, J.M., Nayfeh, A.H., Mook, D.T., 1989. Development of an analytical model of wing rock for slender delta wings. AIAA Journal of Aircraft 26, 737–743.

Ioannou, P.A., Sun, J., 1996. Robust Adaptive Control. Prentice-Hall, Englewood Cliffs, NJ.

Levin, D., Katz, J., 1984. Dynamic load measurements with delta wings undergoing self-induced roll oscillations. AIAA Journal of Aircraft 21, 30–36.

Nayfeh, A.H., Elzebda, J.M., Mook, D.T., 1989. Analytical study of the subsonic wing-rock phenomenon for slender delta wings. AIAA Journal of Aircraft 26 (9), 805–809.

Nounou, H.N., 2003. Adapting the direction of the search vector for direct adaptive continuous-time nonlinear systems. In: Proceedings of the IEEE Conference on Decision and Control, Maui, HI, December 2003, pp. 2890–2895.

Nounou, H.N., Passino, K.M., 2004. Stable auto-tuning of adaptive fuzzy/neural controllers for nonlinear discrete-time systems. IEEE Transactions on Fuzzy Systems 12.

Sastry, S., Bodson, M., 1989. Adaptive Control: Stability, Convergence, and Robustness. Prentice-Hall, Englewood Cliffs, NJ.

Sastry, S.S., Isidori, A., 1989. Adaptive control of linearizable systems. IEEE Transactions on Automatic Control 34, 1123–1131.

Spooner, J.T., Passino, K.M., 1996. Stable adaptive control using fuzzy systems and neural networks. IEEE Transactions on Fuzzy Systems 4, 339–359.

Wang, L.-X., 1994. Adaptive Fuzzy Systems and Control: Design and Stability Analysis. Prentice-Hall, Englewood Cliffs, NJ.